Advances in Military Technology
Vol. 21, No. 1, 2026, pp. 95-112
ISSN 1802-2308, eISSN 2533-4123
DOI 10.3849/aimt.02012

Investigation of the Mechanical Dynamics of the PRV-1 Machine Gun Installed on a Combat Robot

L. Thanh Tuan[1], N. Thai Dung[1], and Vu Duong[2*]

[1] *Department of Weapons, Le Quy Don Technical University, Hanoi, Vietnam*
[2] *School of Engineering Technology, Duy Tan University, Da Nang, Vietnam*

The manuscript was received on 11 July 2025 and was accepted after revision for publication on 17 March 2026.

Abstract:

This paper investigates dynamics of a PRV-1 machine-gun mounted on a combat robot using multi-body mechanics and finite-element approaches. A model quantifies gas pressure forces on the barrel base and piston face, including a damping mechanism. Structural dynamics were solved by two methods: differential equations of motion solved in Maple and dynamic equivalence modeling in MSC Adams. Results – presented as time histories of displacement and velocity for the bolt carrier, gun body, and robot – agree methods and match observed operational behavior. The analysis demonstrates the critical role of the damping system in reducing recoil and improving accuracy, identifies key dynamic parameters for optimization, and provides a scientific basis for designing and optimizing weapon systems on future platforms, as well as guiding future experimental validation efforts.

Keywords:

robot-weapon system, damping mechanism, recoil force, optimization of weapon system, multi-objective learning method

1 Introduction

Today, along with the continuous development of science and technology in all fields of social life including the field of military science, great achievements have been achieved. One of the most significant ones is the technology that allows minimizing the presence of people on the battlefield. The installation of automatic guns on combat robots is a trend to perform tasks to ensure the safety of soldiers in special combat spaces. However, this combination must comply with strict military-technical requirements, including the requirements for stability and especially the firing accuracy

* *Corresponding author: School of Engineering Technology/Duy Tan University, Da Nang, Vietnam. Phone: +84 913 931 101, E-mail: vuduong@duytan.edu.vn*

of the weapon. Therefore, the investigation of the dynamics of the robot-weapon system in combat is an important basis for building the structural parameters of the robot to satisfy the actual tasks set.

In the world, in addition to the development of weapons with high legality and aerial operation, foreign military experts also research and develop combat robots. Combat robots are divided into two main types: autonomous combat robots and controlled combat robots. Alongside the development of highly lethal airborne weapons, foreign military experts are researching and developing combat robots. Autonomous combat robots are robots that are capable of operating on their own in a region, identifying their own targets, and firing without human intervention. Controlled combat robots, after reconnaissance detects the target, have their firing decided by the operator at the control station. Some typical types of robots are the Russian Platform-M robot, the American Talon Sword robot, and Israel's Typhoon system [1] and [2].

[3] presents a method to determine the parameters to evaluate the firing stability of the howitzer mounted on wheeled vehicles. The dynamic model is established based on Newton's law of motion. The model consists of 2 rigid bodies with 5 degrees of freedom. The 105 mm howitzer M101 mounted on the wheeled vehicle Ural-375 is selected for the dynamic model simulation. This paper also presents a method for calculating the recoil resistance and applies the dynamic analysis of recoiling parts of the 105 mm Howitzer M101 when it is recoiling. The results in this paper are used to test the firing stability of the howitzer mounted on wheeled vehicles. This is also a scientific basis that can be used in research and design calculations to optimize the structure of the artillery-vehicle complex. In [4], dynamic simulations are run and their results are compared with matching experimental data to validate the model; the method is applied to computational and experimental studies of Russia's BM-21 system.

In [5], the mathematical model of a 12-degree-of-freedom (DOF) light armored vehicle is introduced, consisting of eight degrees of vertical freedom of movement of eight tires, three degrees of freedom of vertical movement, rolling and tilting of the hull, and one degree of freedom of angular movement of the turret relative to the weapon platform. The two sources of interference considered in this study are uneven lines and jet force at the weapon mount. The research results show that the active suspension system based on stability enhancement can significantly improve the dynamic performance of light armored vehicles compared with passive systems. The article [6] deals with the vibrations of the main parts of the weapon system where the automatic cannons are mounted. The dynamic model has 8 DOF with three parts: hull, turret, and elevation parts. The presented procedure can evaluate the possible changes of the elevation angles, like the aiming errors during the variation of the dynamic characteristics, for example, the masses, mass moment of inertia, stiffness, damping coefficients, and weapon operation principle. The sensitive analysis was applied on the system.

The study [7] examines the effects of arm construction, arm mounting location, and firing angle on the vibration response of the body tube in special vehicles and unmanned vehicles. Unlike traditional two-degree-of-freedom combat robots, this paper establishes a rigid-flexible coupled dynamic model for a new three-degree-of-freedom combat robot to investigate the response characteristics of its body tube during movement. To accurately reflect the driving conditions of the mobile robot, a road surface unevenness model was established using the sine wave superposition method. The firing accuracy of a small combat robot can be affected by the speed and road conditions, as shown in numerous studies.

[8] investigates the crashworthiness of the developed TAERO UGV using finite element method (FEM) analysis. Descriptions of the LS-DYNA simulation model, material properties, and boundary conditions are provided. The primary objective was to numerically assess the bumper performance during impact, considering the operational speeds and crumple zone of the vehicle. An optimized numerical model was introduced to efficiently simulate vehicle collisions, focusing on key structural elements. The presented numerical analysis indicates that impacts with typical obstacles, like tree trunks in unstructured terrain, cause minimal damage, not affecting the operational vehicle capability. Minor bumper damage, such as dents, varies and is more noticeable at higher speeds, while almost imperceptible up to 25 km/h. Stress distribution highlights the role of side components in energy absorption and structural deformation. The results confirm the structural integrity of the vehicle and provide valuable data on its operation performance in complex environments during specialized missions.

To improve computational efficiency, the Next-Generation NATO Reference Mobility Model (NG-NRMM), an accelerated global mobility prediction method, DSAM, is proposed [9]. Unlike previous studies that focused solely on terrain modeling or computational acceleration, DSAM introduces a dual-strategy synergy that combines data-driven FE-DE coupling with adaptive soil patch computation to achieve order-of-magnitude simulation speedup. Specifically, this method enhances simulation efficiency through two primary strategies. First, in terrain modelling, a data-driven FE-DE coupling approach to overcome the computational dimensionality challenges inherent in DE simulations is introduced. Second, in simulation computation, the authors propose a non-complete moving soil patch method combined with multi-CPU parallel processing to substantially improve the real-time performance of mobility simulations. Experiments using real terrain data show that DSAM significantly improves prediction efficiency while maintaining accuracy.

In scientific research, some studies have used the multi-object system mechanics method to investigate the stability problem of weapons-price systems. [10] deals with the vibration of automatic weapons mounted on a tripod in the event of a shot. The theoretical part creates a spatial model of the dynamics of a multibody system using the method of Lagrange equations of motion, which considers the influence of the terrain and the human body. The model has been experimentally verified on the 30 mm AGS-17 grenade launcher. The obtained results are the basis for evaluating the fire stability of an automatic weapon when firing in bursts, which allows modernization of existing weapons and their new use by troops, such as further vehicle mounts, Navy and Coast Guard vessels, and helicopters, as well as evaluation of similar weapon systems.

[11] deals with the analysis of the automatic weapon firing stability mounted on the tripod. The dynamic model has eight degrees of freedom. Three degrees of freedom represent translational motion of the weapon, and three degrees of freedom belong to the rotational motion with the gravity center. The last motions are shooter displacement and the vibration of the elevation parts. The method can evaluate the possible changes of the elevation angles, firing height, and weapon operation principle.

In [12], a new twin-barrel gun model for calculating firing on the elastic ground to study the effects of structural parameters on the weapon's performance is proposed. This paper intends to provide a theoretical basis and establish a specific model of a twin-barrel gun, to build a system of differential equations of vibration, and to determine the rules of vibration of the gun when firing on the elastic ground. The method is used to establish a model of two sets of automatic firing systems by dynamics of a multi-body system. The results of the calculation revealed the instructional significance for improving the vibration performance and increasing the firing accuracy.

In Vietnam, to implement the project "Research on integration of existing weapons into motor vehicles for day and night combat", the Institute of Mechanization Engineering has implemented the project "Research and calculation on the design, manufacture, installation, and testing of 105 mm cannon and 12.7 mm anti-aircraft machine gun integrated into Ural-432007-10 military transport vehicles". In 2017, the Institute of Technology developed, manufactured, and launched a multipurpose autonomous robot for reconnaissance and ground combat, capable of operating under harsh conditions. In 2014, the Le Quy Don University carried out the project "Research on the installation of 12.7 mm anti-aircraft machine guns of the NSV type and 82 mm mortars on PCF ships".

However, there are very few studies on the dynamics of weapon systems mounted on mobile platforms that simultaneously employ multibody mechanics methods and dynamic simulation methods to assess the accuracy of their results. This research aims to evaluate the stability of an automatic gun mounted on a combat robot by using both computational approaches.

2 Developing a Model for Calculating and Surveying the Dynamics of the Robot-Weapon System

2.1 Basic Hypotheses

Based on analyzing the principle of operation and the properties of the gun-robot system with a recoil reduction mechanism, the following assumptions are accepted:

- The mechanism is a system of many objects. The mechanisms of the gun are absolute solid objects made up of some parts.
- The mass of objects in the system is the mass of distribution replaced by the concentrated mass and placed at the center of the object.
- Consider the body parts, sighting mechanism, and gun mount to be rigid and rigidly locked during firing; the links are considered ideal, without gaps.
- The effect of the gun box on the rack through the recoil damper, making the gun box move in a linear direction with the coefficients K_{gg}, B_{gg}.

2.2 Robot-Weapon System Calculation Model Using Multi-Object Learning Method

The system consists of four objects: object 1, including the body, the sight part, and the gun rack, with a mass of m_1; object 2, the barrel of the gun, with a volume of m_2; object 3, the basic stage, with a volume of m_3; and object 4, the working stage of the automatic machine, with a shift depending on the movement of the base stage. Within the framework of the article, we consider the barrel lock (Fig. 1). The paper is considered in the vertical plane, and the correlation between objects is simultaneous in a system. To survey, we use coordinate systems: the fixed coordinate system $Ox_0y_0z_0$ is attached to the O_0 center of gravity of the vehicle before firing. The dynamic coordinate system $Ox_1y_1z_1$ is attached to the body, $Ox_2y_2z_2$ is attached to the barrel, $Ox_3y_3z_3$ is attached to the barrel lock platform, and $Ox_4y_4z_4$ is attached to the barrel lock. The direction of the coordinate axes is shown in Fig. 1.

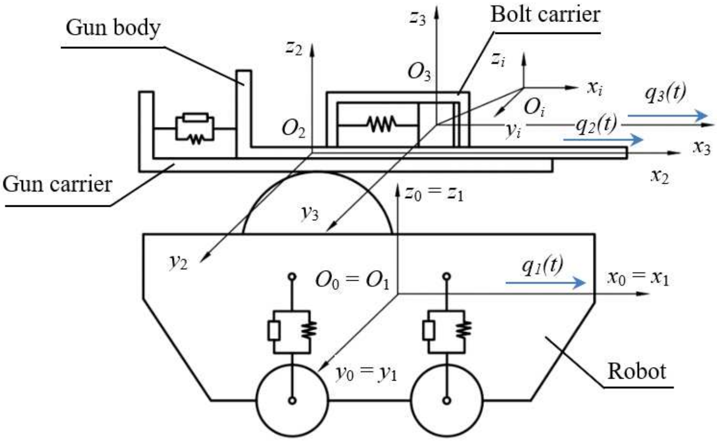

Fig. 1 Model of mechanical system

Within the framework of the content of the article, the author considers the movements of the system as follows: the robot has a gun holder in stop mode. The gun body m_2 is linked to the robot mount m_1 via a sliding joint and shock absorber, which has a transitional motion along the O_2x_2 axis relative to the robot. The barrel lock platform (base stitching) m_3 slides along the barrel m_2, so there is a ramp shift along the O_3x_3 axis. The barrel lock m_4 (working stitching) moves in the directional groove on the barrel and is linked to the base stitch line.

To analyze the firing fluctuations of the gun when mounted on the robot, the study simplifies the computational model while maintaining the accuracy of the mechanism under investigation. The system is described using the following generalized coordinates (degrees of freedom): transitional displacement of the body's center of gravity q_1 along O_1x_1; transitional movement of the gun box q_2 along O_2x_2; transitional displacement of the barrel lock platform's center of gravity q_3 along O_3x_3; and transitional movement of the lock platform's center of gravity q_4 along O_4x_4.

A system of differential equations describing the motion of a system using the Lagrange method has the form [13, 14]:

$$\frac{\mathrm{d}}{\mathrm{d}t}\left(\frac{\partial T_\Sigma}{\partial \dot{q}_j(t)}\right)-\frac{\partial T_\Sigma}{\partial q_j(t)}=Q_j, \quad j=1\div 4\,,\ j=1\div 4 \tag{1}$$

where T_Σ – the total kinetic energy of the system; Q_j – the generalized forces acting on objects; q_j – the coordinates of the deduction.

The structural simulation model using the dynamic simulation method in MSC Adams software was presented in Fig. 2.

3 Solving the Problem of Robot-Weapon Mechanical Dynamics

3.1 Determination of Mechanical Kinetic Energy, Possible Work and Amplification Forces

The kinetic energy of a system is determined as the total kinetic energy of objects:

$$T_\Sigma = T_1 + T_2 + T_3 + T_4 \tag{2}$$

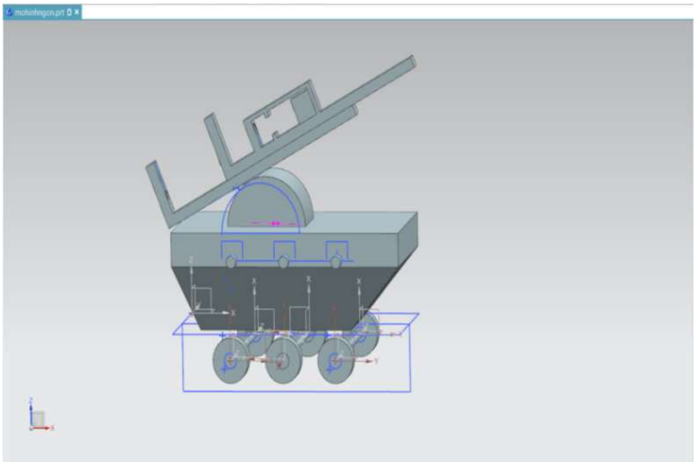

Fig. 2 Structural simulation model in MSC Adams software

where

$$T_1 = \frac{1}{2}\dot{R}_1^{\mathrm{T}} m_1 \dot{R}_1 \text{ – the kinetic energy of the robot,}$$

$$T_2 = \frac{1}{2}\left(\dot{R}_2^{\mathrm{T}} m_2 \dot{R}_2 + \omega^{\mathrm{T}} A_0^2 I_2 A_0^{3\mathrm{T}} \omega\right) \text{ – the kinetic energy of the gun body,}$$

$$T_3 = \frac{1}{2}\left(\dot{R}_3^{\mathrm{T}} m_3 \dot{R}_3 + \omega^{\mathrm{T}} A_0^3 I_3 A_0^{3\mathrm{T}} \omega\right) \text{ – the kinetic energy of bolt carrier,}$$

$$T_4 = \frac{1}{2}\left(\dot{R}_4^{\mathrm{T}} m_4 \dot{R}_4 + \omega^{\mathrm{T}} A_0^4 I_4 A_0^{4\mathrm{T}} \omega\right) \text{ – the kinetic energy of the bolt mechanism.}$$

R_1, R_2, R_3, R_4, m_1, m_2, m_3, m_4 represent the center vector and mass matrix of the robot, gun body, bolt carrier, and bolt mechanism in the O_0 fixed coordinate system. I_2, I_3, I_4 represent the inertia tensor of the gun body for the axle system in the coordinate system O_2, the bolt carrier in the coordinate system O_3, and the bolt mechanism in the coordinate system O_4:

$$\left.\begin{aligned}
\boldsymbol{R}_1 &= [q_1 \quad 0 \quad 0]^{\mathrm{T}} \\
\boldsymbol{R}_2 &= \boldsymbol{R}_1 + \boldsymbol{A}_0^2 \times \boldsymbol{U}_1^2 \\
\boldsymbol{R}_3 &= \boldsymbol{R}_2 + \boldsymbol{A}_0^3 \times \boldsymbol{U}_2^3 \\
\boldsymbol{R}_4 &= \boldsymbol{R}_3 + \boldsymbol{A}_0^4 \times \boldsymbol{U}_3^4 \\
\boldsymbol{\omega} &= \boldsymbol{A}_0^3 \times [0 \quad \dot{q}_2 \quad 0]^{\mathrm{T}} \\
\boldsymbol{U}_1^2 &= [a_{21} \quad b_{21} \quad c_{21}]^{\mathrm{T}} \\
\boldsymbol{U}_2^3 &= [a_{32} + q_3 \quad b_{32} \quad c_{32}]^{\mathrm{T}} \\
\boldsymbol{U}_3^4 &= [a_{43} + q_4 \quad b_{43} \quad c_{43}]^{\mathrm{T}}
\end{aligned}\right\}$$

where $\boldsymbol{A}_0^2, \boldsymbol{A}_0^3, \boldsymbol{A}_0^4$ – the matrices are transferred from the static coordinate axis systems O_2, O_3, and O_4 into the fixed coordinate axis system O_0,

$\boldsymbol{U}_1^2, \boldsymbol{U}_2^3, \boldsymbol{U}_2^4$ – are accordingly original vectors O_2 in the axis system O_1, original vector in the axis system O_3 in the axis system O_2, original vector O_4 in the axis system O_3:

$$\left.\begin{aligned} \boldsymbol{A}_0^2 &= \boldsymbol{A}_1^2 \\ \boldsymbol{A}_0^3 &= \boldsymbol{A}_0^2 \times \boldsymbol{A}_2^3 \end{aligned}\right\}$$

$\boldsymbol{A}_1^2, \boldsymbol{A}_2^3, \boldsymbol{A}_3^4$ – accordingly, are the rotating matrices from coordinate axis systems O_2 to O_1, O_3 to O_2 and O_4 to O_3:

$$\boldsymbol{A}_1^2 = \begin{bmatrix} 1 & 0 & 0 \\ 0 & 1 & 0 \\ 0 & 0 & 1 \end{bmatrix}$$

$$\boldsymbol{A}_2^3 = \begin{bmatrix} \cos q_2 & 0 & \sin q_2 \\ 0 & 1 & 0 \\ -\sin q_2 & 0 & \cos q_2 \end{bmatrix}$$

$$\boldsymbol{A}_3^4 = \begin{bmatrix} \cos \alpha & 0 & \sin \alpha \\ 0 & 1 & 0 \\ -\sin \alpha & 0 & \cos \alpha \end{bmatrix}$$

α – the deviation angle of the direction of movement of the bolt mechanism stitch relative to one of the axes of the axis system O_3.

The total virtual work of the generalized forces is calculated according to the formula:

$$\delta W = \delta WP + \delta WF_{\text{ts}} + \delta WF_{\text{dm}} + \delta WP_{\text{pg}} + \delta WP_{\text{gc}} + \left(\sum_{k=1}^{4} \delta WF_{\text{w}k}\right) + \delta WF_{\text{mr}} + \delta WF_{\text{ar}} \quad (3)$$

where δWP, δF_{ts}, δF_{dm}, δWP_{pg}, δWP_{gc}, $\delta W_{\text{w}k}$ (k = 1,⋯, 4), δWF_{mr}, and δWF_{ar} are respectively the virtual work of gravity, the force of the thrust spring, the force of the recoil damping mechanism, the propellant gas force, the force of the gas pressure in the gas chamber acting on the gun, the elastic force of the wheels, the resistance force of the magazine, and the auxiliary resistance force of the automatic machine [15, 16], in which:

- $\delta WP = \sum_{i=1}^{4} \delta WP_i + \delta WP_{\text{m}} + \delta WP_{\text{b}}$ – the virtual work of gravity,
- $\delta WP_i = P_i^{\text{T}} \delta R_{iz}$ ($i = 1 \div 4$) – the virtual work of gravity of objects 1, 2, 3, 4,
- $\delta WP_{\text{m}} = P_{\text{m}}^{\text{T}} \delta R_{\text{m}z}$ – the virtual work of magazine mechanism,
- $\delta WP_{\text{b}} = P_{\text{b}}^{\text{T}} \delta R_{\text{b}z}$ – the virtual work of bolt,
- $\delta R_{iz} = \sum_{j=1}^{4} \frac{\partial R_{iz}}{\partial q_j} \delta q_j$; $\delta R_{\text{m}z} = \sum_{j=1}^{4} \frac{\partial R_{\text{m}z}}{\partial q_j} \delta q_j$; $\delta R_{\text{b}z} = \sum_{j=1}^{4} \frac{\partial R_{\text{b}z}}{\partial q_j} \delta q_j$ – the virtual movement of the center of gravity of objects 1, 2, 3, and 4; the magazine mechanism; and the bolt.

- $\delta WF_{\text{ts}} = -F_{\text{ts}}\left(\delta R_{\text{ts}}^2 - \delta R_{\text{ts}}^3\right)$ – the virtual work of the force of the thrust spring,
- $F_{\text{ts}} = K_3\left(f_{30} + q_3\right)$ – the compression force of the recoil spring,
- $\delta R_{\text{ts}}^2 = \sum_{j=1}^{4} \frac{\partial R_{\text{ts}}^2}{\partial q_j}\delta q_j$; $\delta R_{\text{ts}}^3 = \sum_{j=1}^{4} \frac{\partial R_{\text{ts}}^3}{\partial q_j}\delta q_j$ – the virtual movement of the points of force on objects 2 and 3,
- f_{30} – the spring compression corresponding to position $q_3 = q_{30}$,
- $\delta WF_{\text{dm}} = F_{\text{dm}}\delta R_2$ – the virtual work of the force of the recoil damping mechanism,
- $F_{\text{dm}} = K_{\text{dm}}\left(f_{20} - q_2\right)$ – the compression force of recoil damper spring; f_{20} – the initial compression corresponds to the balanced position before firing,
- $\delta WP_{\text{pg}} = P_{\text{pg}}^{\text{T}}\delta R_{\text{pg}}$ – the virtual work of the propellant gas force,
- P_{pg} – the pressure force of the propelled gas is calculated according to the system of internal discharge equations,
- $\delta R_{\text{pg}} = \sum_{j=1}^{4} \frac{\partial R_{\text{pg}}}{\partial q_j}\delta q_j$ – the virtual movement of the point of force P_{pg},
- $\delta WP_{\text{gc}} = P_{\text{gc}}^{T}\left(\delta R_{\text{gc}}^3 - \delta R_{\text{gc}}^4\right)$ – the virtual work of the force of the gas pressure in the gas chamber acting on the gun,
- P_{gc} – the pressure force of the propeller gas in the gas chamber is determined according to the thermodynamic equation system of the gas chamber,
- $\delta R_{\text{gc}}^3 = \sum_{j=1}^{4} \frac{\partial R_{\text{gc}}^3}{\partial q_j}\delta q_j$; $\delta R_{\text{gc}}^4 = \sum_{j=1}^{4} \frac{\partial R_{\text{gc}}^4}{\partial q_j}\delta q_j$ – the virtual movement of the points of application of the forces P_{gc} in the moving coordinate frames O_3 and O_4,
- $\delta WF_{\text{w}k} = F_{\text{w}k}\delta R_{\text{w}k}$ – the virtual work of elastic force $F_{\text{w}k}$ at the wheel k,
- $F_{\text{w}k} = \boldsymbol{A}_{0z}^{1} F_{\text{w}k1}$ – the force applied at the wheel k,
- $\delta R_{\text{w}k} = \sum_{j=1}^{4} \frac{\partial R_{\text{w}k}}{\partial q_j}\delta q_j$ – the virtual movement of the point of force $F_{\text{w}k}$,
- $\boldsymbol{A}_{0z}^{1}$ – the matrix rotating around the z-axis from the O_1 axis system to the O_0 axis system,
- $F_{\text{w}k1}$ – the force applied at the k wheel in the O_1 axis system,
- $\delta WF_{\text{mr}} = F_{\text{mr}}^{\text{T}}\delta R_{\text{mr}}$ – the virtual work of magazine resistance force,
- F_{mr} – the magazine resistance,
- $\delta R_{\text{mr}} = \sum_{j=1}^{4} \frac{\partial R_{\text{mr}}}{\partial q_j}\delta q_j$ – the virtual movement of the resistance point of the magazine,
- $\delta WF_{\text{ar}} = -F_{\text{ar}}^{\text{T}}\left(\delta R_{\text{ar}}^3 - \delta R_{\text{ar}}^4\right)$ – the virtual work of the auxiliary resistance force of the automatic mechanism,

- F_{ar} – the auxiliary resistance of the automatic machine includes ejection resistance, resistance to withdrawal and casing withdrawal, and friction on the slides,
- $\delta R_{\mathrm{ar}}^3 = \sum_{j=1}^{4} \frac{\partial R_{\mathrm{ar}}^3}{\partial q_j} \delta q_j$; $\delta R_{\mathrm{ar}}^4 = \sum_{j=1}^{4} \frac{\partial R_{\mathrm{ar}}^4}{\partial q_j} \delta q_j$ – the virtual movement of the auxiliary resistance point on object 3 in the O_3 coordinate system and of object 4 in the O_4 coordinate system.

3.2 Solving the Problem of Internal Launch and Thermodynamics of the Gas Chamber

To determine the force of the gas pressure acting in the barrel, we need to solve the problem of internal launch. Different methods can be used; here the author uses the method of integrating the number of differential equation systems. The differential equation system of the inner ejection problem is expressed as follows [17]:

$$\begin{cases} \dfrac{\mathrm{d}v}{\mathrm{d}t} = \xi_1 \xi_3 \dfrac{pS}{\varphi m} \\ \dfrac{\mathrm{d}l}{\mathrm{d}t} = \xi_1 \xi_3 v \\ \dfrac{\mathrm{d}z}{\mathrm{d}t} = \xi_2 \dfrac{p}{I_k} \\ \dfrac{\mathrm{d}\omega_c}{\mathrm{d}t} = \xi_2 \chi \omega (1 + 2\lambda z) \dfrac{p}{I_k} - \xi_{\mathrm{ac}} G_b - (1 - \xi_3) G_d \\ \dfrac{\mathrm{d}w}{\mathrm{d}t} = \xi_2 \dfrac{1 - \alpha\delta}{\delta} \chi \omega (1 + 2\lambda z) \dfrac{p}{I_k} + \xi_3 s v \\ \dfrac{\mathrm{d}p}{\mathrm{d}t} = \dfrac{1}{w} \left\{ \left[\xi_2 \dfrac{p \chi \omega}{I_k} \left(f - K_p \dfrac{1 - \alpha\delta}{\delta} \right) (1 + 2\lambda z) - K_p S v \xi_3 \right] - \right. \\ \qquad \left. - K_p \left[\xi_b G_b + (1 - \xi_3) G_d \right] - K_t p \right\} \end{cases} \tag{4}$$

where K_t – the function to determine heat loss which is determined as follows:

$$K_t = \frac{(k-1) A \nu_1 \sigma_{\mathrm{T}} \left(F_k + \pi d l \right)}{R}$$

A – the thermomechanical equivalents [J]; F_k – the initial surface area of the ammunition chamber [m^2]; d – the caliber [m]; l – the distance of movement of the bullet in the barrel [m]; R – the gas constant, [J·mol^{-1}K^{-1}]; σ_{T} – the heat transfer coefficient [W·m^{-2}·K^{-1}].

$$\nu_1 = \frac{T_{\mathrm{is}}}{T^0}$$

where T_{is} – the inner surface temperature of barrel [K]; T^0 – the propeller gas temperature, [K]. Function to determine a flow rate:

$$K_p = \frac{kpw}{\omega}$$

v – the bullet velocity [m·s^{-1}]; p – the propeller gas pressure [Pa]; S – the cross-sectional area of the barrel [m^2]; φ – the virtual factor of bullet mass; α – the propeller gas generation capacity [m^3·kg^{-1}]; δ – the specific weight of propeller [kg·m^{-3}]; F – the propellant force [N]; k – the multivariate index; w – the volume of space behind the bullet bottom [m^3]:

$$w = w_0 + Sl$$

w_0 – the initial volume of the bullet chamber [m^3]; m – the bullet mass [kg]; ω – the propellant weight [kg]; ω_c – the weight of propellant gas [kg]; I_k – the momentum of propellant gas pressure [N·s]; χ, λ – the propellant shape characteristics; z – the relative thickness of propellant particles; G_b – the air flow into the air chamber [kg·s^{-1}]; G_d – the air flow through the muzzle of barrel [kg·s^{-1}];

$$\begin{cases} G_b = \mu_\varphi S_{\varphi i} \sqrt{\dfrac{p\omega_c}{w}} \left[\xi_4 A_1 + (1-\xi_4) A_2 A_2(\beta)\right] \\ G_d = \mu S \sqrt{\dfrac{p\omega_c}{w}} \left[\xi_d A_1 + (1-\xi_d) A_2 A_2(\beta)\right] \end{cases} \tag{5}$$

where

$$A_1 = \sqrt{gk\left(\frac{2}{k+1}\right)^{\frac{k+1}{k-1}}} \text{ and } A_2 = \sqrt{\frac{2kg}{k-1}} \text{ – loss factors,}$$

$$A_2(\beta) = \sqrt{\beta^{\frac{2}{k}} - \beta^{\frac{k+1}{k}}} \text{ – loss function,}$$

$$\beta = \frac{p_1}{p_2}$$

where p_1, p_2 – the pressure in the chamber in which the drug gas flows in and out; g – the gravity acceleration, [m·s^{-2}]; $S_{\varphi i}$ – the gas extraction hole area [m^2]; ξ_1 – the control coefficient that determines when the projectile begins to move after the cartridge link is severed; ξ_2 – the control coefficient that determines the time at which the propellant has completely burned; ξ_3 – the control coefficient that determines the time at which the projectile exits the barrel; ξ_i – the control coefficient that determines when the projectile nose has passed the gas port on the barrel wall.

The coefficients are determined according to Tab. 1.

Tab. 1 Coefficients ξ_i in the internal ballistic calculation

ξ	ξ_1		ξ_2		ξ_3		ξ_i	
value	1	0	1	0	1	0	1	0
condition	$p > p_0$	$p < p_0$	$z < 1$	$z \geq 1$	$l < l_d$	$l \geq l_d$	$l \geq l_i$	$l < l_i$

p_0 – the bullet belt cutting pressure [Pa]; l_d – the length of the barrel with twist groove [m]; l_i – the location of the air extraction hole from the end of the twist groove [m]; ξ_4, ξ_d – the control coefficients used to solve the thermodynamics of the gas chamber.

With $\beta_{gh} = \left(\dfrac{2}{k+1}\right)^{\frac{k}{k+1}}$, coefficients ξ_4, ξ are determined according to Tab. 2.

Tab. 2 Values ξ_4 and ξ_d

ξ_4		ξ_d	
1	0	1	0
$\beta \leq \beta_{gh}$	$\beta > \beta_{gh}$	$\beta \leq \beta_{gh}$	$\beta > \beta_{gh}$

3.3 Determination of the Force Applied to the Gas Extraction Device

The system of equations describes the thermodynamic process in the gas chamber based on the basic processes of aerodynamics as follows:

$$\begin{cases} \dfrac{\mathrm{d}\omega_b}{\mathrm{d}t} = \xi_i \left(G_b - G_{\mathrm{ac}} \right) \\ \dfrac{\mathrm{d}w_b}{\mathrm{d}t} = \xi_i \left(\dot{X} S_b \right) \\ \dfrac{\mathrm{d}p_b}{\mathrm{d}t} = \xi_i \dfrac{1}{w_b} \left(kRTG_b - kRT_b - kp_b w_b \right) \end{cases} \tag{6}$$

where ω_b – the weight of the propellant gas flowing into the gas chamber [kg]; w_b – the volume of propellant gas occupying a place in the gas chamber, [m^3]; S_b – the cross-sectional are of piston head [m^2]; p_b – the pressure in the gas chamber [kg·m^{-2}]; $\dot{X}$ – the velocity of the bolt carrier [m·s^{-1}]; T_b – the temperature in the gas chamber [K]; G_{ac} – the air flow through the gap between cylinder and piston of the air chamber [kg·s^{-1}]:

$$G_{\mathrm{ac}} = \mu_k S_\Delta A_1 \sqrt{\frac{p_b \omega_b}{w_b}}$$

where S_Δ – the area of the gap between piston and gas chamber cylinder [m^2]; μ_k – the loss coefficient (μ_k = 0.3–0.5).

This system of equations is solved simultaneously with the system of Eq. (4).

3.4 Solving the Problem of Robot-Weapon Mechanism Dynamics

The system of differential equations to solve the dynamic problem of the system includes the system of differential equations that describes the movement of the system, the system of internal launch differential equations of PRV-1 machine guns, and the system of thermodynamic equations of gas chambers. The input data to solve the internal launch technique problem and the air chamber thermodynamic problem of PRV-1 guns are obtained according to the document [18]. Robot-weapon system inputs are taken from model simulation data on Autodesk Inventor graphics software: P_1 = 1 000 N; P_2 = 200 N; P_3 = 75.5 N; P_4 = 8.6 N; P_m = 0.75 N; P_b = 1.47 N; J_{1xx} = 1.667 kg·m^2; J_{1yy} = 2.833 kg·m^2; J_{1zz} = 3.234 kg·m^2; J_{2xx} = 0.018 kg·m^2; J_{2yy} = 0.018 kg·m^2; J_{2zz} = 0.014 kg·m^2; J_{3xx} = 0.01 kg·m^2; J_{3yy} = 0.27 kg·m^2; J_{3zz} = 0.269 kg·m^2; J_{4xx} = 0.00014 kg·m^2; J_{4yy} = 0.009 kg·m^2; J_{4zz} = 0.008 kg·m^2; $J_{\mathrm{m}xx} = J_{\mathrm{m}yy} = J_{\mathrm{m}zz}$ = 325.10^{-7} kg·m^2; $J_{\mathrm{b}xx} = J_{\mathrm{b}yy} = J_{\mathrm{b}zz}$ = 926.10^{-8} kg·m^2. The spring stiffness of the robot's shock absorber: $K_{\mathrm{w}x}$ = 800 N·m^{-1}; the stiffness of recoil damper spring: K_{dm} = 300 N·m^{-1}; the stiffness of the thrust spring back: K_3 = 4 N·m^{-1}. The

 DOI 10.3849/aimt.02012

coordinates of the center of gravity of objects are determined according to the system simulation software.

Maple software is used to simultaneously solve dynamic equation systems, including differential equations that describe motion, internal discharge processes, and the thermodynamic behavior of the gas chamber. As a result, we obtain the law of gas pressure, the law of movement of bullets, the law of air chamber pressure, the law of movement of automatic machines, and the law of movement of the mechanism during firing.

Figs 3 and 4 show the results of the internal launch and thermodynamics of the gun's air chamber when firing.

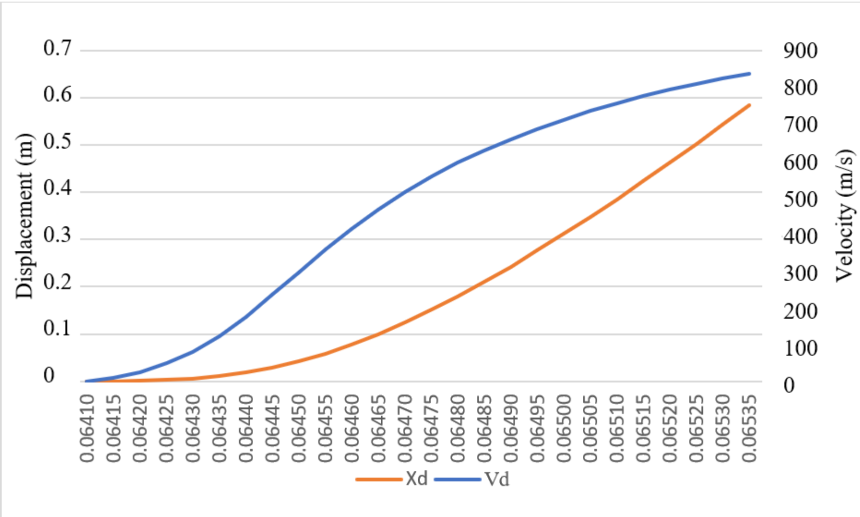

Fig. 3 Graph of bullet displacement and velocity in the barrel

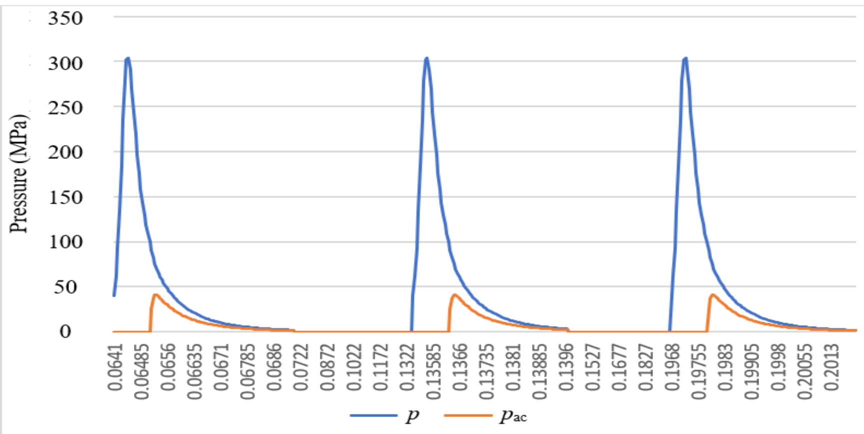

Fig. 4 Graph of internal ballistics pressure for three consecutive shots

The results of the calculation of the internal launch technique and the thermodynamics of the gas chamber are relatively close to the test results of previous research works and the manufacturer's official documents. Specifically, the maximum pressure value in the barrel is 304.363 MPa; according to the manufacturer's documentation, it is 305 MPa, and the error is 0.3 %. The calculated muzzle velocity is 837.2 m·s^{-1}; according to the manufacturer's documentation, it is 825 m·s^{-1}, the error is 0.15 %.

Fig. 5 shows the displacement and velocity of the bolt carrier when firing at an angle of about 0°. The firing cycle time is 0.0924 s, which corresponds to a theoretical rate of fire of 648 rounds per minute. The rate of fire recorded in the equipment manual is 650 rounds per minute. The calculated rate of fire is relatively consistent with the published references and the manufacturer's documentation.

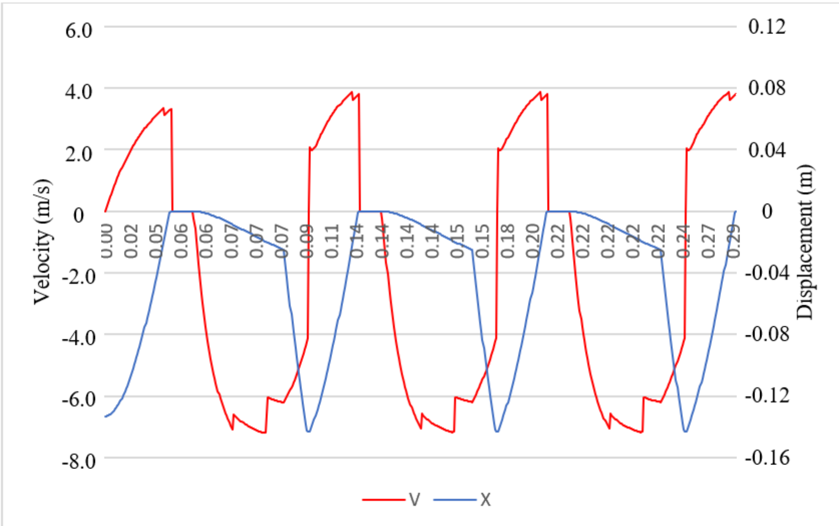

Fig. 5 Graph of displacement and velocity of the bolt carrier

Figs 6a, 6b shows the displacement and velocity of the gun body when firing at an angle of about 0°. Regarding the oscillation of the barrel, the results show that the dis-placement of the barrel relative to the price through recoil reduction depends on the initial preliminary parameter of the recoil reduction. The working cycle of the recoil absorber when installing the recoil absorber spring as calculated is smaller than the working cycle of the automatic machine, ensuring refueling, so the work between different shots will not have too much difference in the position of the gun barrel.

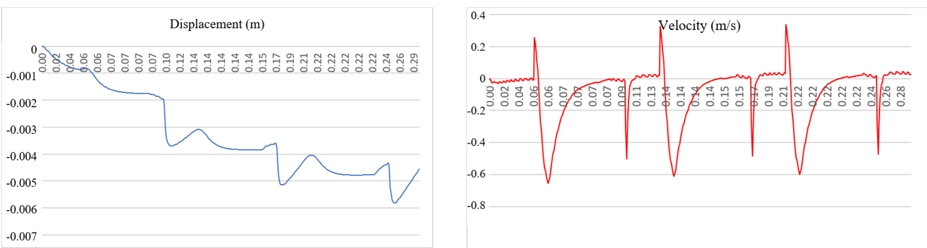

a) *b)*

Fig. 6 Graph of displacement and velocity of the gun body:
a – displacement; b – velocity

Figs 7a, 7b shows the displacement and velocity of the vehicle platform, and Figs 8a, 8b shows the roll and pitch angle of the robot body when firing at an angle of about 0°. In terms of body oscillation, the displacement of the body compared to the fixed coordinate system depends on the weight of the whole block and the friction at the wheels. The force acting on the wheels is the sum of the forces caused by the mass of gravity and the forces generated by the shot.

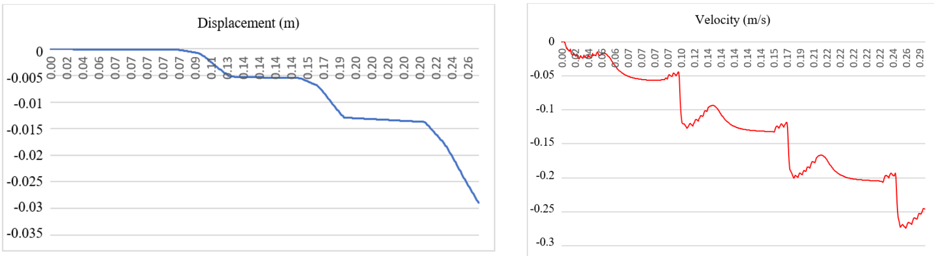

a) *b)*

Fig. 7 Graph of displacement and velocity of the vehicle platform:
a – displacement; b – velocity

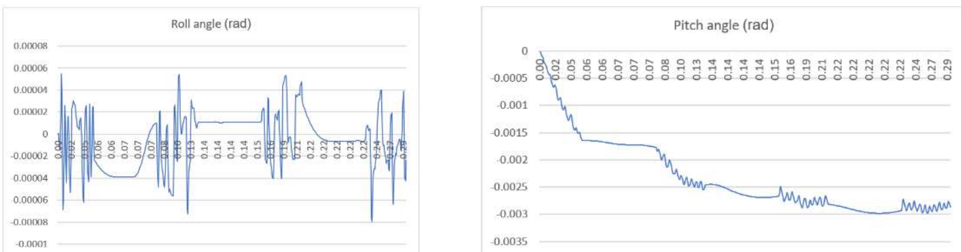

a) *b)*

Fig. 8 Graph of roll and pitch angle of the vehicle platform:
a – roll angle; b – pitch angle

The survey results of firing the gun on the robot at different elevations and azimuth angles show that the time-history vibration plots during firing are relatively similar. When firing at an elevation angle of 30°, the displacement of the links is greater compared to an elevation angle of 0°, but the difference is insignificant. When firing at different azimuth angles, the oscillation angle is larger compared to an azimuth angle of 0°, but the difference is relatively small.

3.5 Simulation of System Dynamics Using Dynamic Simulation Method

Based on the model developed in MSC Adams – with parameters for element dimensions and layout conforming to the PRV-1 cannon's construction – the simulation verifies the mechanism's behavior and confirms that the gun functions according to its designed operating principle. The input values correspond to the initial data of the problem when surveyed by the mechanical method of multi-body systems. The external force acting on the mechanism includes the force exerted by the pressure of the gas on the bottom of the barrel and the force for the pressure of the gas extraction applied to the piston obtained from the results of the internal launch and thermodynamic problems of the gas chamber. The results of the corresponding mechanical dynamics analysis are shown in Figs 9–12.

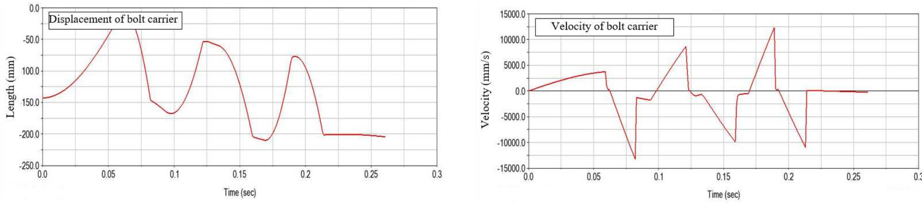

a) *b)*

Fig. 9 Graph of displacement and velocity of the bolt carrier:
a – displacement; b – velocity

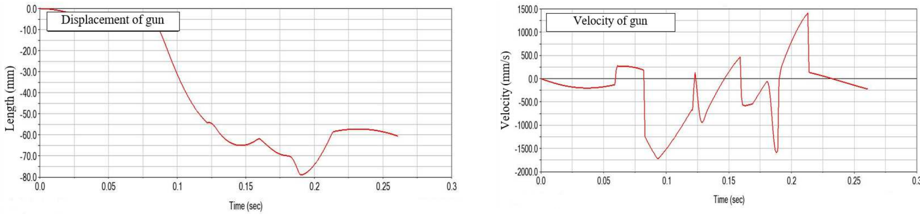

a) *b)*

Fig. 10 Motion graph of displacement and velocity of the gun body:
a – displacement; b – velocity

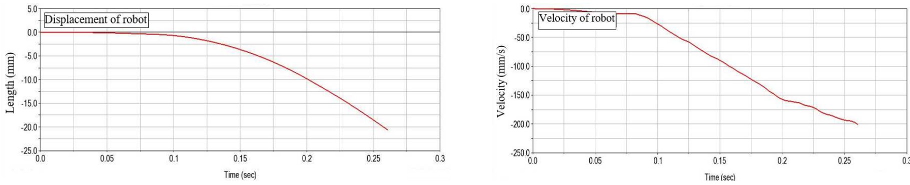

a) *b)*

Fig. 11 Motion graph of displacement and velocity of the vehicle platform:
a – displacement; b – velocity

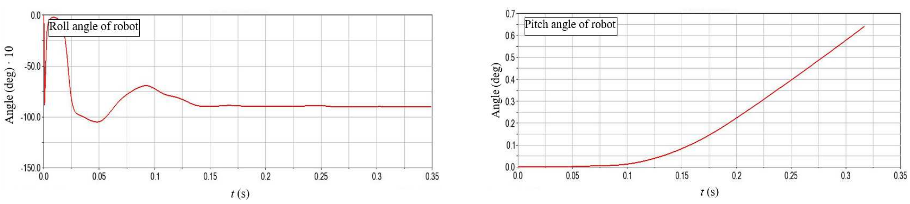

a) *b)*

Fig. 12 Motion graph of roll angle and pitch angle of the vehicle platform:
a – roll angle; b – pitch angle

Through the research process, it was observed that the two methods – the multi-body mechanics method and the dynamic simulation method – produce results that exhibit a distinct geometric similarity between their respective plots. Since the links are rigidly connected to each other, the oscillatory motion of the links depends on the sway angle of the vehicle body. Therefore, the specific results focus on the motion of the vehicle body along the *Ox* axis and on the roll angle and pitch angle of the vehicle body. Specifically:

- motion along the *Ox* axis: according to the problem solved using the multibody mechanics method, the displacement at the considered time is $x_{\mathrm{hmax}} = 0.028$ m; the simulation results give the displacement at the same time as $x_{\mathrm{hmax}} = 0.021$ m,
- roll (lateral oscillation): according to the problem solved using the multibody mechanics method, the roll angle at the considered time is $\psi_{\mathrm{hmax}} = 0.00008$ rad; the simulation results give the roll angle at the same time as $\psi_{\mathrm{hmax}} = 0.00002$ rad,
- pitch (longitudinal oscillation): according to the problem solved using the multibody mechanics method, the pitch angle at the considered time is $\theta_{\mathrm{hmax}} = 0.0031$ rad; the simulation results give the pitch angle at the same time as $\theta_{\mathrm{hmax}} = 0.006$ rad.

It can be observed that the maximum values obtained from the simulation method are relatively close to those from the multibody mechanics method. However, there is a certain margin of error. The main reasons can be summarized as follows:

- The simulation model was built in its most simplified form as blocks of defined shapes, whereas the gun consists of many components and working surfaces that affect the motion during firing, primarily through resistance forces caused by impacts.
- In the process of dynamic calculation of the simulation model, the interactions between the components were considered with force coefficients (without assuming them to be perfectly rigid bodies).

4 Conclusion

Based on building a robot-weapon mechanism model, using the mechanical theory of the multi-object system, a system of differential equations of motion of the PRV-1 machine gun automatic machine mounted on a combat robot was built through a spring-loaded recoil reduction mechanism. By the numerical method in conjunction with the internal launch equation system, the thermodynamic equation system of the air chamber was employed to determine the displacements of the gun body, vehicle body, and barrel lock platform during firing. The calculation results obtained from the multi-body mechanical method were then validated and compared with those of the corresponding model analyzed using the finite element method, simulated in Adams software. The calculation results are relatively consistent with theoretical data, ensure a certain reliability, and can be used as a basis for studying the dynamics of weapons mounted on combat robots as well as when calculating the design, improvement, and optimization of the system. The research results provide a basis for developing automatic control systems for weaponized robots that can autonomously track and engage targets. This enables enhanced safety and reduced casualties among soldiers on the battlefield and during special missions.

Acknowledgment

This work did not receive any financial support outside.

References

[1] SIWEK, M. and K. WACŁAWIK. Legal Aspects of Production and Operation of Autonomous Combat Robots. *Problems of Mechatronics Armament, Aviation, Safety Engineering*, 2020, **11**(2), pp. 81-94. DOI 10.5604/01.3001.0014.1995.

[2] STHIYANARAYANAN, M., S. AZHARUDDIN, S. KUMAR and G. KHAN. Self Controlled Robot for Military Purpose. *International Journal for Technological Research in Engineering*, 2014, **1**(10), pp. 1075-1077. ISSN 2347-4718.

[3] BIEN, V.V., L. DOBSAKOVA, N. VAN DUNG, D.P. NGUYEN, T.D. NGUYEN and M.P. NGUYEN. A Study on Firing Stability of Howitzer Mounted on Wheeled Vehicles. In: *2023 International Conference on Military Technologies (ICMT)*. Brno: IEEE, 2023. DOI 10.1109/ICMT58149.2023.10171322.

[4] BIEN, V.V, M. MACKO, N.T. DUNG, N.D. PHON, N.T. HAI and B.T. TUAN. Dynamic Simulation Analysis and Optimization of Firing Rate of Rocket Launchers on Wheeled Vehicles. *Advances in Military Technology*, 2021, **16**(1), pp. 159-175. DOI 10.3849/aimt.01459.

[5] HUDHA, K., H. JAMALUDDIN and P.M. SAMIN. Disturbance Rejection Control of a Light Armoured Vehicle using Stability Augmentation Based Active Suspension System. *International Journal of Heavy Vehicle Systems*, 2008, **15**(2), pp. 152-169. DOI 10.1504/IJHVS.2008.022240.

[6] BALLA, J. Dynamics of Mounted Automatic Cannon on Track Vehicle. *International Journal of Mathematical Models and Methods in Applied Sciences*, 2011, **5**(3), pp. 423-432.

[7] GAO, X., X. GUAN, K. ZOU, Z. WANG and J. KANG. Research on Body Tube Vibration Response of Small Combat Robots Motion. *Mathematical Problems in Engineering*, 2023, **2023**(1), 7425844. DOI 10.1155/2023/7425844.

[8] NOWAKOWSKI, M. and K. KOSIUCZENKO. Evaluation of TAERO UGV Structural Collision Resistance Using FEM Analysis. *Bulletin of the Polish Academy of Sciences, Technical Sciences,* 2025, **73**(3), e153431. DOI 10.24425/bpasts.2025.153827.

[9] HUA, C., Y. WEI, C. JIANG and R. NIU. DSAM: Dual-Strategy Simulation Acceleration-Based Model for Unmanned Ground Vehicle Mobility Prediction. *IEEE Transactions on Vehicular Technology,* 2025, **74**(11), pp. 16667-16678. DOI 10.1109/TVT.2025.3574523.

[10] BIEN, V.V., J. BALLA, H.M. DAO, H.T. TRUONG, D.V. NGUYEN and T.V. TRAN. Firing Stability of Automatic Grenade Launcher Mounted on Tripod. In: *2021 International Conference on Military Technologies (ICMT)*. Brno: IEEE, 2021. DOI 10.1109/ICMT52455.2021.9502836.

[11] BALLA, J., M. HAVLICEK, L. JEDLICKA, Z. KRIST and F. RACEK. Dynamics of Automatic Weapon Mounted on the Tripod. *Advances in Mathematical and Computational Methods*, 2014, pp. 122-127. ISSN 1792-6114.

[12] DOAN, D.V. A Study on Multi-Body Modeling and Vibration Analysis for Twin-Barrel Gun While Firing on Elastic Ground. *Applied Engineering Letters*, 2023, **8**(1), pp. 36-43. DOI 10.18485/aeletters.2023.8.1.5.

[13] WITTENBURG, J. *Dynamics of Multibody Systems*. 2nd ed. Berlin: Springer, 2008. ISBN 978-3-540-73913-5.

[14] SHABANA, A.S. *Dynamics of Multibody Systems.* 5th ed. New York: Cambridge University Press, 2020. ISBN 978-1-108-48564-7.

[15] BIEN, V.V. *Dynamics Model of Small Automatic Weapon System Mounted on a Fighting Robot When Firing* (in Vietnamese). *Journal of Science and Technology*, 2025, **61**(1), pp. 72-80. DOI 10.57001/huih5804.2025.011.

[16] DERBY, S.J. *Design of Automatic Machinery*. Boca Raton: CRC Press, 2004. ISBN 0-429-13165-8.

[17] THE, D.N., T.D. NGOC and D.N. NGOC. Internal Ballistic Calculations of the Solid Propellant Rocket Engine with Two Combustion Chambers. *Journal of Science and Technique*, 2021, **16**(3), pp. 109-122. ISSN 1859-0209.

[18] TUAN, L.T. The Survey of Dynamics of Robot-Weapon System Based on Mechanics of Multi-Body System. *Journal of Military Science and Technology*, 2021, **72**, pp. 150-157. ISSN 1859-1043.